URSI GASS 2021, Rome, Italy, 28 August - 4 September 2021

Incident Power Density Assessment of Smart Surfaces for Exposure Compliance

Sen Liu* (1), Teruo Onishi (1), Masao Taki (1), and Soichi Watanabe(1)
(1) National Institute of Information and Communications Technology, Tokyo, Japan, 184-8795, E-mail: liusen@nict.go.jp

Abstract

This paper presents preliminary research on the compliance assessment of smart surfaces, which are one of the most promising technologies for 5G higher frequency band (NR2) applications. Two different approximate approaches are provided and compared with the reference approach, which is based on full-wave simulation, in terms of assessment accuracy and efficiency to verify their availability and capability quantitatively. Both the two approximate approaches can significantly reduce the assessment time while providing acceptable assessment accuracy.

1 Introduction

5G wireless communications will make full use of high frequency band up to millimeter wave to provide ultra-high data rate transmission, consequently leading to unprecedented challenges in RF chain design [1]. Hybrid Beamforming [1] that combines analog/digital beamforming techniques could be a potential solution, however, with limited performance. Alternatively, smart surfaces [2] that consist of hundreds of reconfigurable elements to produce desired scattering characteristics (e.g.: multi-/shaped-beams) can largely relax the system design while providing full service coverage and have attracted much attention recently.

All devices that radiate electromagnetic fields (EMFs) are required to comply with the relevant regulatory requirements on human exposure. The two most widely referred exposure guidelines are those issued by ICNIRP [3] and IEEE [4]. Both guidelines provide frequency-specified exposure limits based on decades of scientific research and suggest incident power density as exposure metric at 28 GHz, which represents the typical 5G NR2 frequency band.

In this paper, the compliance assessment of simplified smart surfaces that is composed of non-reconfigurable elements is investigated. The purpose is to quantitatively verify the two presented approximate assessment approaches. Specifically, two different approximate approaches for radiation pattern calculation are provided. Then, the compliance boundary and front compliance distance are derived according to the far-field spherical formula [5] for each obtained pattern and compared with the reference approach, which is based on full-wave simulation, in terms of assessment accuracy and computation time.

2 Assessment Approaches

2.1 Front Compliance Distance

Smart surfaces working as radio base station antennas are expected to be deployed in the area where the public is located in the far-field region. Besides, with edge illumination taper around -10 dB compared with the center taper, which is usually the case for smart surfaces, the highest exposure is normally toward the front direction. Correspondingly, the front compliance distance defining as the front boundary outside of which the exposure level is below the exposure limits is of particular interest and considered here. The incident power density can be easily calculated once the radiation patterns of the smart surfaces are given, and then is compared with the exposure limits to determine the compliance boundary and the corresponding front compliance distance. Therefore, efficiently obtaining accurate radiation patterns is particularly helpful for compliance assessment.

2.2 Radiation Pattern Calculation

Three different approaches for radiation pattern calculation are provided and briefly discussed in the following.

2.2.1 Array-Theory Approach

Due to the array nature of smart surfaces, array theory formulation can be applied, where the formula is shown in the following: [6-7]

$$E(\theta,\varphi)=\sum_M\sum_N A_{mn}\cdot R_{mn} \cdot \mathbf{cos}^{q_e}(\theta)\cdot e^{j\cdot k\cdot \bar{r}_{mn}\cdot\hat{u}} \quad (1)$$

in which A_{mn} represents the incident field distribution (obtained by full-wave simulation), R_{mn} denotes the reflection response (obtained by periodic boundary condition with normal incidence of fundamental Floquet modes), $\mathbf{cos}^{q_e}(\theta)$ is the scalar approximation of the radiation pattern of the element, q_e describes the power factor of the element (usually equal 1 for half-wavelength element), $\hat{u} = (\hat{x}\sin\theta\cos\varphi, \hat{y}\sin\theta\sin\varphi, \hat{z}\cos\theta)$ is the observation direction, and $\vec{r}_{mn}$ is the position vector of the mnth element. With appropriate numerical operation, the evaluation of the double summation in (1) can be significantly accelerated using Fast Fourier Transform (FFT) algorithm. It should be noticed that the radiation pattern is obtained in angular coordinates (u, v) and only in the forward hemisphere. Then, radiation integral expression [8] is used to determine the gain pattern of the smart surfaces.

2.2.2 Equivalent-Current Approach

Alternatively, by calculating the electrical/magnetic current distribution on the surface, equivalent principle can be applied [9-10]. The electric and magnetic current are defined as:

$$\begin{cases} \vec{\mathbf{J}}_s = \hat{n} \times \vec{\mathbf{H}} \\ \vec{\mathbf{M}}_s = -\hat{n} \times \vec{\mathbf{E}} \end{cases} \tag{2}$$

where $\vec{\mathbf{H}}$ and $\vec{\mathbf{E}}$ represent the total magnetic and electric fields on the surface, and are usually obtained for element by element with the consideration of the actual incident angle assuming local periodicity. Besides, with half-wavelength periodicity, only fundamental Floquet modes need to be considered since all the high-order modes are evanescent modes that do not contribute to the far-field radiation. Once the current distribution on the surface is constructed, near-field to far-field transformation expressions [8] are used to obtain the radiation pattern in the entire sphere. Here, due to continuous field distribution for each element, FFT algorithm cannot be applied.

2.2.3 Reference Approach

Reference approach denotes the numerical modelling of the entire smart surface using full-wave algorithms (e.g.: FDTD, MoM, and FEM) that can precisely calculate the actual mutual coupling between elements, edge diffraction, and feed blockage, and is the most accurate approach, however, with significantly higher computation time and resources compared with the above approaches. All the relative errors in the following are calculated based on the results obtained in reference approach.

3 Results

3.1 System Configuration and Radiation Patterns Comparison

The system configuration used for verification is summarized in Table I. The smart surface is designed to produce a pencil beam toward $\theta_b = 30^\circ$ and $\varphi_b = 45^\circ$ as shown in the Fig. 1. Half-wavelength square-patch element that has been widely introduced [11] is used here

TABLE I
SYSTEM CONFIGURATION

Frequency	28 GHz
Surface diameter	112.6 mm
Element number	305
Substrate thickness	0.8 mm
Relative permittivity (ε_r)	2.2
Feed offset angle	$\theta_F = 30^\circ$, $\varphi_F = 180^\circ$
Distance from feed to surface center	95 mm
Main beam direction	$\theta_b = 30^\circ$, $\varphi_b = 45^\circ$
Input power	50 W

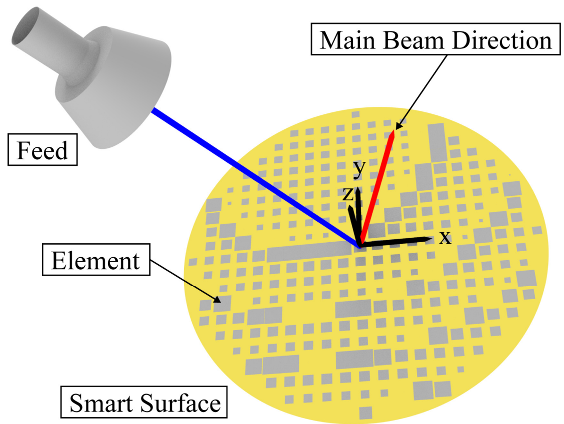

Fig. 1 System configuration illustration.

to provide desired compensation phase. The source feed is a corrugated horn antenna with a -10 dB beamwidth of 60.9° and a gain of 14.9 dBi, providing edge taper from -7.2 dB to -11.7 dB.

The radiation patterns obtained using the three approaches described in Section 2 at $\varphi = 45^\circ$ plane are depicted in Fig. 2. Compared with the result from array-theory approach, the result based on equivalent-current approach demonstrates improved accuracy in terms of gain calculation.

3.2 Front Compliance Distance Comparison

Once the radiation patterns are computed, the incident power density at specific coordinates is calculated based on far-field spherical formula [5] shown below:

$$S = \frac{P \cdot G}{4\pi r^2} \tag{3}$$

in which S is incident power density [W/m^2], P is input power [W], G is the antenna gain, and r is the distance between the antenna and evaluation point. Then, it is compared with the exposure limits to determine the front compliance distance. Table II lists the corresponding results. Both equivalent-current approach and array-

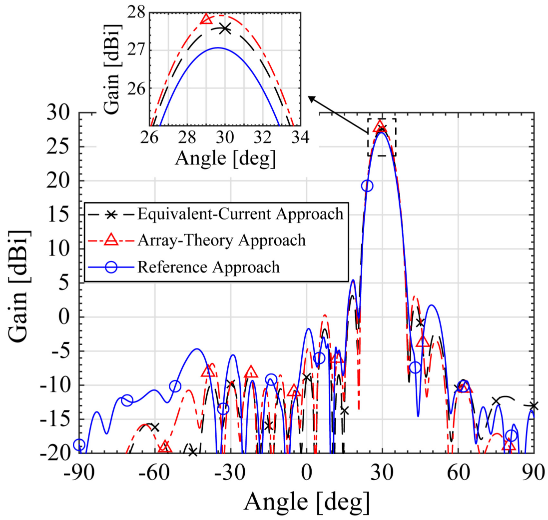

Fig. 2 Radiation patterns cut at $\varphi = 45^{\circ}$ plane.

TABLE II
FRONT COMPLIANCE DISTANCE COMPARISON

Approach	Front compliance distance [m]	Relative error [%]	Computation time [%]*
Equivalent-Current	13.1	6.50	14.1
Array-Theory	13.6	10.57	14.0
Reference	12.3		100 (23758 sec)

* It represents the relative evaluation time compared with the reference for the entire assessment process including all the prerequisite data computation (e.g.: incident field distribution, element reflection response, etc.).

theory approach show significantly reduced computation time compared with reference approach. It should be mentioned that the evaluation time of the two approximate approaches for the case of considering all the possible beam conditions will show much more improvement than that of reference approach since the two approximate approaches actually share some same prerequisite data that only need to be calculated once. Relative errors of 6.50% and 10.57% are obtained for equivalent-current approach and array-theory approach, respectively, which are generally acceptable for compliance assessment. It should be noticed that the compliance distance evaluated by the approximate approaches are larger than the reference, denoting conservative evaluation, which is mainly due to the fact that the calculated gain using the approximate approaches are slightly higher than the reference.

4 Conclusion

In this paper, the compliance assessment of smart surfaces, which are one promising technology for 5G higher frequency band (NR2) applications, was investigated. Two approximate approaches, namely array-theory approach and equivalent-current approach, were presented and compared with the reference approach that is based on full-wave simulation, in terms of assessment accuracy and time consumption. It was shown that both the two approximate approaches could largely save the assessment time while providing assessment accuracy of relative error < 11%, which is generally acceptable for compliance assessment. Further studies are required to prove the full availability for the two approximate approaches on compliance assessment of smart surfaces.

5 Acknowledgements

This work was supported by the Ministry of Internal Affairs and Communications (JPMI10001) in Japan.

6 References

[1] I. Ahmed, H. Khammari, A. Shahid, A. Musa, K. S. Kim, E. D. Poorter, and I. Moerman, "A Survey on Hybrid Beamforming Techniques in 5G: Architecture and System Model Perspectives," *IEEE Commun. Surveys Tuts.*, vol. 20, no. 4, pp. 3060-3097, 4th Quart. 2018.

[2] S. Gong, X. Lu, D. T. Hoang, D. Niyato, L. Shu, D. I. Kim, and Y.-C. Liang, "Toward Smart Wireless Communications via Intelligent Reflecting Surfaces: A Contemporary Survey," *IEEE Commun. Surveys Tuts.*, vol. 22, no. 4, pp. 2283-2314, 4th Quart. 2020.

[3] ICNIRP, "Guidelines for Limiting Exposure to Electromagnetic Fields (100 kHz to 300 GHz)," *Health Phys.*, vol. 118, no. 5, pp. 483-524, 2020.

[4] *IEEE Standard for Safety Levels with Respect to Human Exposure to Electric, Magnetic, and Electromagnetic Fields, 0 Hz to 300 GHz*, IEEE Standard C95.1-2019, 2019.

[5] *Determination of RF field strength, power density and SAR in the vicinity of radiocommunication base stations for the purpose of evaluating human exposure*, International Electrotechnical Commission Std. 62232, Aug. 2017, Ed. 2.0.

[6] D. M. Pozar, S. D. Targonski, and H. D. Syrigos, "Design of Millimeter Wave Microstrip Reflectarrays," *IEEE Trans. Antennas Propag.*, vol. 45, no. 2, pp. 287-296, Feb. 1997.

[7] R. C. Hansen, *Phased Array Antennas*. New York, NY, USA: Wiley, 1998.

[8] C. Balanis, *Antenna Theory: Analysis and Design*. 2nd ed. New York: Wiley, 1997.

[9] Y. Zhuang, K.-L. Wu, C. Wu, and J. Litva, "A Combined Full-Wave CG-FFT Method for Rigorous Analysis of Large Microstrip Antenna Arrays," *IEEE Trans. Antennas Propag.*, vol. 44, no. 1, pp. 102-109, Jan. 1996.

[10] R. F. Harrington, *Time-Harmonic Electromagnetic Fields*. New York: McGraw-Hill, 1961.

[11] J. Huang and J. A. Encinar, *Reflectarray Antennas*. 1st ed. Hoboken, NJ, USA: Wiley, 2008.